Journal of Pathology
J Pathol (2011)
Published online in Wiley Online Library
(wileyonlinelibrary.com) DOI: 10.1002/path.2881

ORIGINAL PAPER

Methyl donor deficiency induces cardiomyopathy through altered methylation/acetylation of PGC-1α by PRMT1 and SIRT1

Maira Moreno Garcia,[1#] Rosa-Maria Guéant-Rodriguez,[1#] Shabnam Pooya,[1#] Patrick Brachet,[2] Jean-Marc Alberto,[1] Elise Jeannesson,[1] Fathia Maskali,[3] Naig Gueguen,[4] Pierre-Yves Marie,[3] Patrick Lacolley,[3] Markus Herrmann,[5] Yves Juillière,[1] Yves Malthiery[4] and Jean-Louis Guéant[1]*

[1] *Inserm U954, Medical Faculty and CHU of Nancy, Nancy University, France*
[2] *Human Nutrition Unit, UMR 1019 INRA/University of Auvergne, INRA Centre of Theix, Saint-Genès Champanelle, France*
[3] *Inserm U961, Medical Faculty and CHU of Nancy, Nancy University, France*
[4] *Inserm U694, Medical Faculty and University of Angers, France*
[5] *Department of Clinical Chemistry and Laboratory Medicine, University Hospital of Saarland, Homburg, Saarland, Germany*

**Correspondence to: Jean-Louis Guéant, Inserm U-954, Faculté de Médecine, 9 Avenue de la Forêt de Haye, B.P. 184, 54500 Nancy-Vandœuvre, France. e-mail: jl.gueant@chu-nancy.fr*

[#]These authors contributed equally to this study.

Abstract

Cardiomyopathies occur by mechanisms that involve inherited and acquired metabolic disorders. Both folate and vitamin B12 deficiencies are associated with left ventricular dysfunction, but mechanisms that underlie these associations are not known. However, folate and vitamin B12 are methyl donors needed for the synthesis of *S*-adenosylmethionine, the substrate required for the activation by methylation of regulators of energy metabolism. We investigated the consequences of a diet lacking methyl donors in the myocardium of weaning rats from dams subjected to deficiency during gestation and lactation. Positron emission tomography (PET), microscope and metabolic examinations evidenced a myocardium hypertrophy, with cardiomyocyte enlargement, disturbed mitochondrial alignment, lipid droplets, decreased respiratory activity of complexes I and II and decreased *S*-adenosylmethionine:*S*-adenosylhomocysteine ratio. The increased concentrations of triglycerides and acylcarnitines were consistent with a deficit in fatty acid oxidation. These changes were explained by imbalanced acetylation/methylation of PGC-1α, through decreased expression of SIRT1 and PRMT1 and decreased *S*-adenosylmethionine:*S*-adenosylhomocysteine ratio, and by decreased expression of PPARα and ERRα. The main changes of the myocardium proteomic study were observed for proteins regulated by PGC-1α, PPARs and ERRα. These proteins, namely trifunctional enzyme subunit α-complex, short chain acylCoA dehydrogenase, acylCoA thioesterase 2, fatty acid binding protein-3, NADH dehydrogenase (ubiquinone) flavoprotein 2, NADH dehydrogenase (ubiquinone) 1α-subunit 10 and Hspd1 protein, are involved in fatty acid oxidation and mitochondrial respiration. In conclusion, the methyl donor deficiency produces detrimental effects on fatty acid oxidation and energy metabolism of myocardium through imbalanced methylation/acetylation of PGC-1α and decreased expression of PPARα and ERRα. These data are of pathogenetic relevance to perinatal cardiomyopathies.

Keywords: cardiomyopathy; epigenetics; fatty acid oxidation; folate; vitamin B12; PGC-1α; PPARα; SIRT1; PRMT1

Received 28 October 2010; Revised 29 January 2011; Accepted 20 February 2011

No conflicts of interest were declared.

Introduction

Cardiomyopathies and heart failure (HF) are major causes of morbidity and mortality in industrialized societies [1]. Cardiomyopathies may occur at the different ages of life, by complex patho-mechanisms that involve inherited and acquired metabolic disorders [1,2]. *S*-adenosylmethionine (SAM) is the universal substrate involved in epigenetics and in the methylation of co-regulators involved in fatty acid oxidation [3]. The methyl donors, folate and vitamin B12 are needed in the one-carbon metabolism for the remethylation of homocysteine (Hcy) into methionine, the direct precursor of *S*-adenosylmethionine [4]. The potential link of methyl donors with the patho-mechanisms of cardiomyopathies is unknown, despite their metabolic role and the high prevalence of the deficiency during perinatality and ageing [4,5]. Several clinical reports and population studies are consistent with such a link. Prenatal dilated cardiomyopathy can be the presenting manifestation of CblC deficiency, an inborn error of intracellular metabolism of vitamin B12 [6]. In very recent years, we and others have shown an association of Hcy and vitamin B12 with left ventricular mass

and left ventricular systolic dysfunction [7,8]. Whether these observations reflect a causative role of methyl donors is a question that needs experimentally-based evidence.

Folate and vitamin B12 act as the co-substrate and the co-factor, respectively, of methionine synthase (MTR). Betaine–homocysteine methyltransferase and cystathionine-ß-synthase being undetectable in cardiomyocytes, they play a limiting role in the synthesis of SAM (see Supporting information, Figure S1) [4,9]. The methyl donor deficiency produces apoptosis and cellular stress in the brain and liver of the deficient rat and in neuronal cells, but its effects on heart fuel homeostasis have not been studied, despite the role of SAM in the activation of peroxisome proliferator-activated receptor-γ co-activator-1 (PGC-1α) [10–13]. PGC-1α functionally interacts with peroxisome proliferator-activated receptor-α (PPARα) and PPARγ, while the activation of PGC-1α depends on methylation by protein arginine methyltransferase-1 (PRMT1) and deacetylation by Sirtuin-1 (SIRT1) [3,13]. The expression of SIRT1 is involved in epigenetic mechanisms of fetal programming, a condition that could be also influenced by the deficiency in methyl donors [3,14]. Finally, PPARα, PPARγ and PGC-1α are three master regulators of the oxidative metabolism of heart mitochondria, which play a central role in the patho-mechanisms that lead to myocardium hypertrophy and heart failure [13,15].

Materials and methods

Animals

Animal treatments were performed according to the National Institutes of Health guide for the care and use of laboratory animals. The review board of Nancy University approved the study. Female Wistar rats (Charles River, Les Oncins, France) were constantly maintained with food and water available *ad libitum*. One month before pregnancy, they were fed either with standard food or with a diet deprived of vitamins B12, folate and choline [10]. Deficient and normal diets were respectively maintained in dams from both groups until weaning of their offspring, occurring 21 days after birth, as described previously [10].

Positron emission tomography (PET) and blood pressure

PET scans and image analysis were performed using an animal small monitoring and gating system M 1025T (Inveon, Siemens Medical, USA). The animals were weighed, anaesthetized and injected with 74 MBq ^{18}F-labelled PEGylated tetrameric RGD Peptide (^{18}F-FPRGD4). PET scans were acquired at 30 min after injection. We drew the regions of interest of each scan using the vendor software (ASI Pro 5.2.4.0, Siemens Medical, Germany). Arterial pressure was measured by tail-cuff plethysmography by using the Hatteras SC-1000 blood pressure analysis system (Hatteras Instruments, USA). The rats were acclimatized to the system for 7 days. The readings were averaged from single sessions of 8–10 acceptable readings.

Morphological analyses and microscope examinations

The 21 day-old rats were killed by decapitation after exposure to halothane and the heart was rapidly removed. At the same time, we examined the body weight and heart weight. Immediately after sacrifice, the hearts were plunged in a solution of cold methyl butane (−30 °C) and stored at −80 °C. Sections (20 µm thick) were serially cut on a cryostat and evaluated in the MCIDTM image analysis system (Cambridge, UK). Cuts of 1.5 µm were contrasted with blue Azur II and observed by optical microscopy. Immunohistochemical analyses were performed on 20 µm heart cryo-sections. For Hcy immunostaining, tissue sections were treated as described [10,14] and incubated overnight at 4 °C with a rabbit polyclonal antibody against Hcy diluted at 1/100 (Chemicon, Temecula, CA, USA). The sections were then incubated for 1 h at room temperature in the presence of a secondary antibody diluted at 1/100 (anti-rabbit IgG conjugated to AlexaFluor; Molecular Probes, Cergy Pontoise, France). For electron microscope examination, freshly isolated hearts were plunged in a solution of 2.5% glutaraldehyde in 0.1 M phosphate buffer, pH 7.4. The tissue was post-fixed in 1% osmium tetroxide, dehydrated in 70–100% ethanol, incubated in propylene oxide, then embedded in Embed 812 resin (Electronic Microscopic Science). Sections of 70–80 nm were observed with a Philips CM12 electron microscope at a magnification of ×45.0 and ×13.0 K. For the specific detection of apoptosis, we used terminal deoxynucleotidyl transferase-mediated dUTP nick-end labelling (TUNEL; Calbiochem, Germany) assay. TUNEL assays were performed as described [10,14], according to the manufacturer's protocol. The fraction of apoptotic cells was determined in five random microscopic fields totalling at least 50 cells/group. The nuclei of apoptotic cells observed were dark brown under the light microscope.

Sample collection of blood and heart tissue and biochemical analyses

Intracardiac blood samples were collected and centrifuged for 10 min at 3000 rpm. Aliquots of plasma were stored frozen at −80 °C until analysis. The heart was rapidly collected, washed in Ringer buffered solution and frozen in liquid nitrogen. Enzymatic activities were determined in whole heart homogenate prepared at 4 °C in 100 mM potassium phosphate buffer, pH 7.3, containing protease inhibitors (proteases inhibitor cocktail; Sigma Chemical Co, St. Louis, MO,

USA). Protein concentration was quantified according to bicinchoninic acid (BCA) protein assay reagent (Pierce, Rockford, USA) with bovine serum albumin as standard. Vitamin B12, folate, Hcy, SAM and *S*-adenosylhomocysteine (SAH) concentrations were determined as described previously [10,12]. The protein concentration of cardiomyocyte homogenates was estimated by BCA assay. Proteins were precipitated with 0.2 N $HCLO_4$, centrifuged and the supernatant was filtered through 0.45 μm before injection on the HPLC column (Lichrospher, 100 RP-C18, 250 × 4 mm i.d., 5 μm film thickness). The concentrations of total and free carnitine and acylcarnitines were measured in heart tissue, as described [16]. Total lipids were extracted and the supernatants were analysed in LC–MS/MS (API 3000, Applied Biosystems, Toronto, Canada). Triglycerides and cholesterol were measured by the enzymatic methods GPO-PAP and CHOD-PAP (Biolabo, Fismes, France) on a multiparametric Automate (Olympus AU400, France).

Analyses in mitochondria

The electron transport chain complexes (complexes I–IV) were measured in isolated mitochondria suspensions as described [17].

Western blotting and immunoprecipitation

Total protein extracts (30 μg) from heart tissue were separated and transferred to PVDF membranes (Millipore, Bedford, MA, USA) as described [10,12,14]. The PVDF membranes were incubated overnight at 4 °C with primary antibodies diluted in TBS buffer containing 5% non-fat dried milk, as follows: anti-Bcl-2 (rabbit polyclonal, 1/2000; Santa Cruz Biotechnology), anti-phospho-ERK 1/2, Thr202/Tyr204 (rabbit polyclonal, 1/2000; Cell Signaling Technology), antiphospho-p38a MAP kinase, Thr108/Tyr182 (rabbit polyclonal, 1/2000; Cell Signaling Technology), anticleaved caspase-3, Asp175 (rabbit polyclonal, 1/2000; Cell Signaling Technology), anti-Bax (rabbit polyclonal, 1/2000; Santa Cruz Biotechnology), anti-PPARα (rabbit polyclonal, 1/700; Cayman), anti-PRMT1 (rabbit polyclonal, 1/700; Cell Signaling Technology), anti-asymmetric dimethylarginine (rabbit polyclonal, 1 : 500; ASYM24, Millipore), anti-SIRT1 (rabbit polyclonal H300, 1/1000; Santa Cruz Biotechnology) and anti-PGC-1α, anti-PPARγ (rabbit polyclonal, 1/1000; Cell Signaling Technology) diluted in TBS buffer containing 5% w/v BSA, TFE/MTPA (mouse monoclonal, 1/2000; Abcom), NDUVF2 (rabbit polyclonal, 1/700; Santa Cruz Biotechnology) and FABP3 (mouse monoclonal, 1/500; Abcom). Appropriate secondary antibodies conjugated to HRP were used for detection with ECL or ECL PLUS reagent (Amersham Pharmacia Biotech, Arlington Heights, IL, USA) and bands were quantified by densitometry using the Image J 5.1 program.

Proteomic analysis of myocardium

Proteomic analysis was essentially carried out as described by Chanson *et al* [11]. Frozen myocardium was pulverized under liquid nitrogen with a mortar and pestle and the resulting powder was homogenized at 4 °C in extraction buffer supplemented with 50 mM DTT instead of tributylphosphine, using a 2 ml all-glass mini-Potter homogenizer. Then, the homogenate was centrifuged at 18 000 × *g* for 15 min and the protein concentration of the supernatant was determined using the RC DC protein assay kit (Bio-Rad Laboratories, Marnes-La-Coquette, France). Extracted proteins (500 μg/gel) were separated by two-dimensional polyacrylamide gel electrophoresis (2D PAGE). Following the second dimension, separate protein spots were visualized on gels by 0.02% w/v colloidal Coomassie blue and images were captured on an image scanner (Amersham, GE Healthcare, Orsay, France). Quantification of protein changes across triplicates of the two conditions analysed was captured via image alignment and analysis, and integrated analysis of expression profiles using the Progenesis SameSpots software (Nonlinear Dynamics, Newcastle upon Tyne, UK). In addition to technical repeats, biological replicates were carried out to address individual variability, using myocardium from six control and six methyl donor-deficient rat pups. Results were expressed as means ± SD. Tailored multivariate statistical analysis facilities incorporated into the Progenesis SameSpots software were used for image analysis, with $p < 0.05$ considered significant. Spots showing a significant change in abundance between the two conditions were subsequently analysed by MALDI–TOF mass spectrometry (Voyager DE-Pro, Perseptive BioSystems, Farmingham, MA, USA) in positive-ion reflector mode for peptide mass fingerprinting (PMF). Differentially expressed proteins were evaluated by Ingenuity Pathways Analysis (Ingenuity System, Mountain View, CA, USA), a software application that enables identification of networks of interacting proteins, based on literature databases and optimized inclusion of as many differentially expressed proteins as possible.

Statistical analyses

Data were analysed with SPSS 17.0 software for Windows (Chicago, IL, USA). Continuous variables were reported as either mean ± SEM or median and quartiles (skewed data distributions). Raw data were compared using one-way analysis of variance (ANOVA). Asterisks denote densitometry data from western blots: $^{*}p < 0.05$; $^{**}p < 0.01$; $^{***}p < 0.001$. In the case of skewed data distributions, logarithmic transformations were carried out to normalize the distributions. Univariate regression analyses were performed with transformed correlation (Fisher *z*-transformation) and Pearson. The minimum level of statistical significance was set at $p < 0.05$.

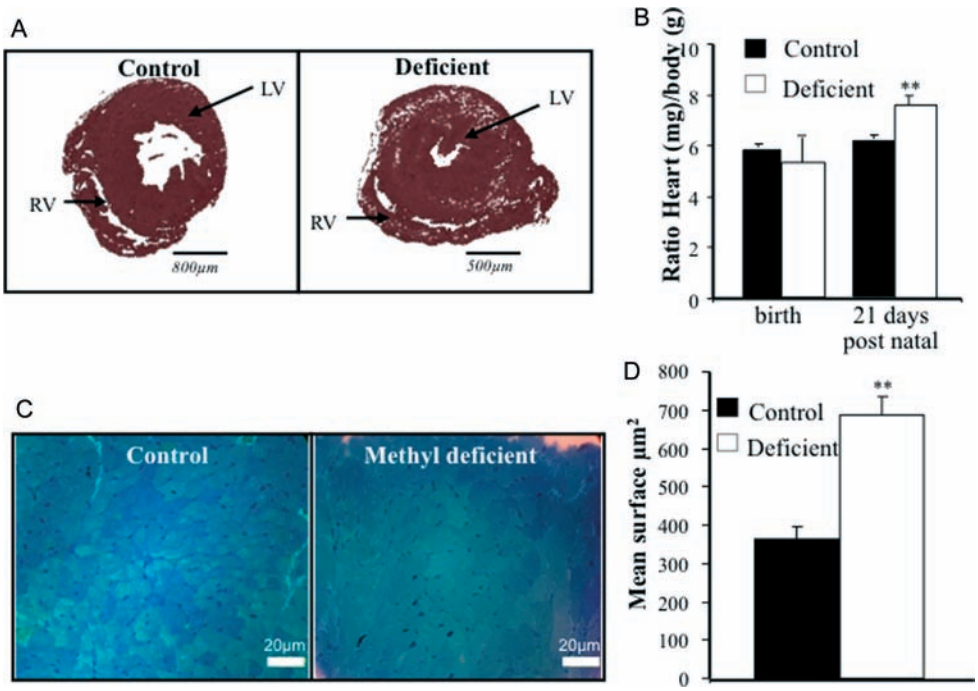

Figure 1. Morphological consequences of the methyl-deficient diet on the myocardium. (A) Microphotographs of 21 day-old rat heart in control condition and methyl deficiency. Bar = 800 µm. LV, left ventricle; RV, right ventricle. (B) Relative heart weight (heart weight : body weight ratio) in control and methyl-deficient rats. (C) Transversely sectioned left ventricle tissue from controls and methyl-deficient rats were stained with blue Azur II and observed with a light microscope. (D) Mean cardiomyocyte surface from control and methyl-deficient rats; 50 myocytes/animal were measured.

Results

The methyl-deficient diet produces a hypertrophy of the myocardium

The body weight of the control pups was significantly lower in the deficient pups compared to the control animals (42.2 ± 2 and 18.4 ± 3.9 g, respectively; $p < 0.001$). The heart weight was also lower (260.2 ± 35.4 and 133.8 ± 39.1 mg, respectively; $p < 0.001$). The deficiency in methyl donors produced a hypertrophy of the ventricular myocardium, evidenced by increased parietal thickness and increased mean surface of cardiomyocytes in the deficient rats compared to controls (Figures 1A–D, 2A). This hypertrophy was developed after birth (Figure 1B), with a 17% increase of the heart weight : body weight ratio in 21 day-old pups (Figure 1B). By comparison, the deficient diet produced a 16% decrease of the stomach size : body weight ratio [14]. The left ventricular ejection fraction (LVEF) was slightly greater in the deficient rats compared to controls, while no significant change was observed for the cardiac frequency and the mean arterial pressure (Figure 2A–C).

The methyl donor-deficient diet decreases folate and SAM : SAH ratio and increases homocysteine in heart tissue

The deficient diet in methyl precursors was effective in decreasing the plasma levels of folate and vitamin B12 and in producing an increase of Hcy in the plasma and the myocardium of deficient pups (Figure 3A, $p < 0.0001$; Figure 3D), as reported previously in other tissues [10,14]. A significant negative correlation was found between the heart weight : body weight ratio and either Hcy ($r = 0.500$, $p = 0.0043$), folate ($r = -0.670$, $p < 0.0001$) or vitamin B12 ($r = -0.609$, $p = 0.0003$). The deficient group exhibited a decreased concentration of folate ($p = 0.0003$) and a paradoxical increased vitamin B12 concentration in heart tissue, compared to controls ($p < 0.0001$) (Figure 3B). A significant increase of SAH was reported in heart tissue, while no significant difference was observed for SAM (Figure 3C). Consequently, the SAM : SAH ratio, which is the limiting determinant of transmethylation reactions, was decreased (Figure 3C).

The methyl donor deficiency alters the mitochondrial/myofibrils alignment and impairs fatty acid oxidation and mitochondria respiration

Microscope examination of the myocardium from the methyl-deficient rats revealed a disturbed mitochondrial alignment along myofibrils and an increased number of lipid droplets, in the absence of any detectable fibrosis (Figure 4A). In agreement with these findings, there was a significant increase in the concentration of triacylglycerol and cholesterol in heart tissue (Figure 4B). A significant increase of plasma short-chain, medium-chain and long-chain acylcarnitines was also detected, reflecting a global deficit in fatty acid oxidation (Figure 4C). The association between the impaired fatty acid β-oxidation, the cardiomyopathy

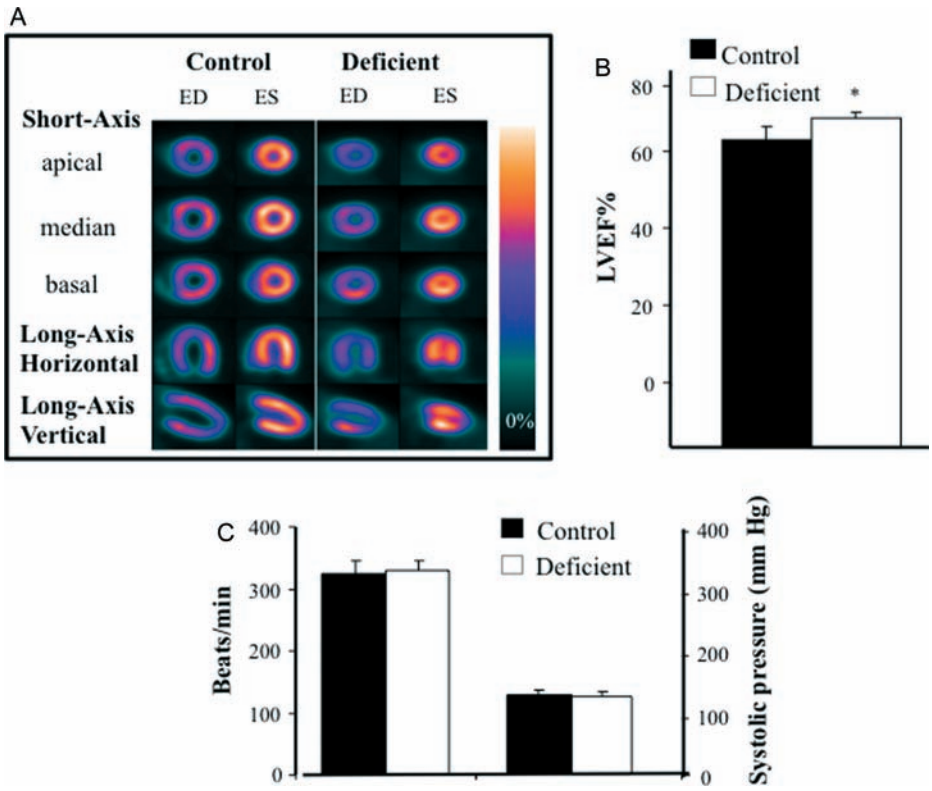

Figure 2. Cardiovascular consequences of the methyl-deficient diet. (A) Images from perfusion and from end-systolic (ES) and end-diastolic (ED) ECG-gated 18F-FDG PET of control and methyl-deficient rats, using an Inveon (Siemens Medical, USA) small-animal PET scanner. (B) Measurement of left ventricular ejection fraction (LVEF). (C) Measurement of systolic pressure by tail-cuff plethysmography, $n = 8$ in each group. Values are mean ± SEM; $^{*}p < 0.05$, $^{**}p < 0.01$, $^{***}p < 0.001$.

and Hcy was also ascertained by significant correlations of acylcarnitines with heart weight : body weight ratio and Hcy. Plasma short-chain, medium-chain and long-chain acylcarnitines correlated with the heart weight : body weight ratio ($r = 0.648$, $p < 0.0001$; $r = 0.660$, $p < 0.0001$; and $r = 0.693$, $p < 0.0001$, respectively) and with Hcy ($r = 0.630$, $p < 0.0001$; $r = 0.733$, $p < 0.0001$; and $r = 0.525$, $p = 0.0005$, respectively). A decreased activity of complexes I and II of the mitochondria respiration was reported in methyl-deficient rats, while no change was observed for complexes III, IV and V (Figure 4D) and for carnitine palmitoyltransferase 1 (CPT1) activity (see Supporting information, Figure S2).

The methyl donor deficiency has no significant consequences on cellular stress and apoptosis

The changes in the alignment and metabolic dysfunctions of mitochondria led us to further investigate the markers of apoptosis and cellular stress. TUNEL assays evidenced no significant increase of apoptosis in the heart tissue of the deficient animals (Figure 5A). Consistently, western analysis found an increased expression of Bcl-2 and a decreased level of cleaved caspase-3 in the heart tissue of the deficient rats (Figure 5B). Western blot analysis showed a decrease in phospho-ERK 1/2 and phospho-p38 MAPK, compared to the respective total proteins, suggesting a lower level of activation of both pathways in the deficient condition (Figure 5C).

Impaired mitochondrial metabolism is related to imbalanced acetylation/methylation of PGC1α and altered expression of PPARα, ERRα and PPARγ

We further investigated PGC1α, PPARα, ERRα and PPARγ, since they act as master regulators of mitochondria metabolism. The myocardium of deficient rats expressed a lower protein level of PPARα and ERRα and a higher level of PPARγ (Figure 6A). In contrast, the expression of PGC-1α was not modified by the deficient diet. We therefore investigated the methylation and acetylation of PGC-1α, two mechanisms that regulate its activity and that may be influenced by the methyl donor deficiency [3,13,14]. The deficient diet produced decreased expression and decreased activity of PRMT1 methyl-transferase (measured by the intracellular levels of its catalytic product, asymmetric dimethylarginine, as described [18]) and of SIRT1 deacetylase and no change of protein expression of GCN5 acetylase (Figure 6B; see also Supporting information, Figure S3). The decreased methylation and the increased acetylation of the immunoprecipitated PGC-1α were the two consequences of the decreased SAM : SAH ratio and of the changes in PRMT1 and SIRT1 expression, which altered PGC-1α activation (Figure 6B).

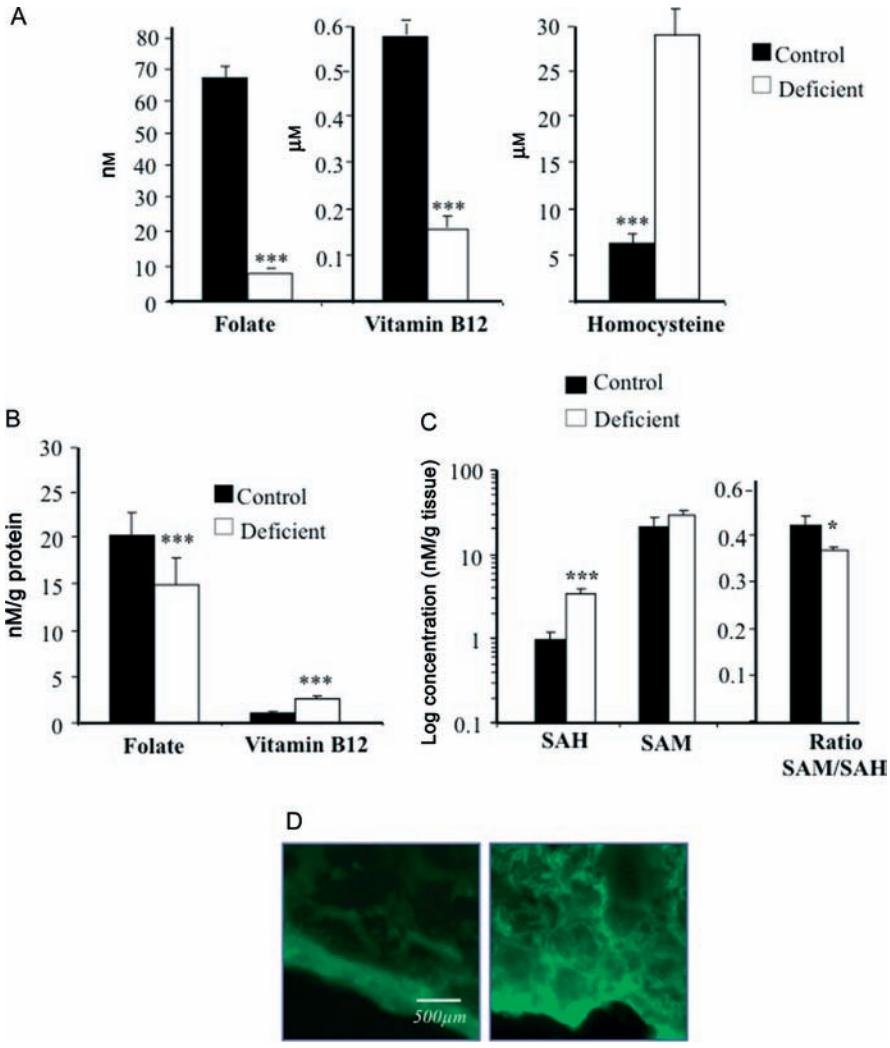

Figure 3. Consequences of the methyl-deficient diet on the one-carbon metabolism in blood and myocardium. (A) Folate, vitamin B12 and homocysteine (Hcy) concentrations in serum of rats. (B) Folate and vitamin B12 concentrations in heart tissue. (C) *S*-Adenosyl-methionine (SAM) and *S*-adenosyl-homocysteine (SAH) concentrations and SAM : SAH ratio in heart tissue. Means ± SEM, $n = 20$ in each group. $^{*}p < 0.05$, $^{***}p < 0.001$. (D) Immunohistochemical identification of homocysteine in rat hearts. Magnification is indicated with bar.

Proteomic analyses evidence altered expression of mitochondrial proteins regulated by PGC1α, PPARα, ERRα and PPARγ

We identified eight proteins related to energy metabolism (and none related with fibrosis) that underwent significantly changed abundance in the myocardium of methyl donor-deficient rat pups compared to their control counterparts. These proteins were the trifunctional enzyme subunit-α complex (TFE-α, also referenced as MTPA or HADHA), short chain acylCoA dehydrogenase (SCAD), the acyl-CoA thioesterase 2 (ACOT2), the fatty acid binding protein-3 (FABP-3, two spots), NADH dehydrogenase (ubiquinone) flavoprotein 2 (NDUFV2), NADH dehydrogenase (ubiquinone) 1α subunit 10 (NDUFA10) and Hspd1 protein (HSPD1), isocitrate dehydrogenase (IDH3A). Representative changes in the spots matching seven of these proteins are illustrated in Figure 7. The Ingenuity Pathways Analysis identified the main changes produced by the methyl donor deficiency as related to transcriptional co-activator PGC-1α, peroxisome proliferator-activated receptor-α (PPARα), oestrogen-related receptor-α (ERRα) and PPARγ (see Supporting information, Figure S4) [18–26]. The decreased magnitude of SCAD spots was related to PPARα and PGC-1α [18,19]. NDUFA10), NDUFV2 and IDH3A were identified as PGC-1α-related [19–23]. Spots matching FABP-3 and TFE-α were identified as ERRα-, PPARα- and PGC-1α-related, ACOT2 as PPARα-related and HSPD1 as PPARγ- and PGC-1α-related [24–27]. The lower expression of TFE-α, SCAD, NDUFV2 and NDUFA10 and increased expression of FABP-3 was confirmed in heart tissue from the deficient rats, compared with control rats (Figure 6C).

Discussion

Our study provides a link between the deficiency in methyl donors, folate and vitamin B12 and the development of myocardial hypertrophy in a well-validated

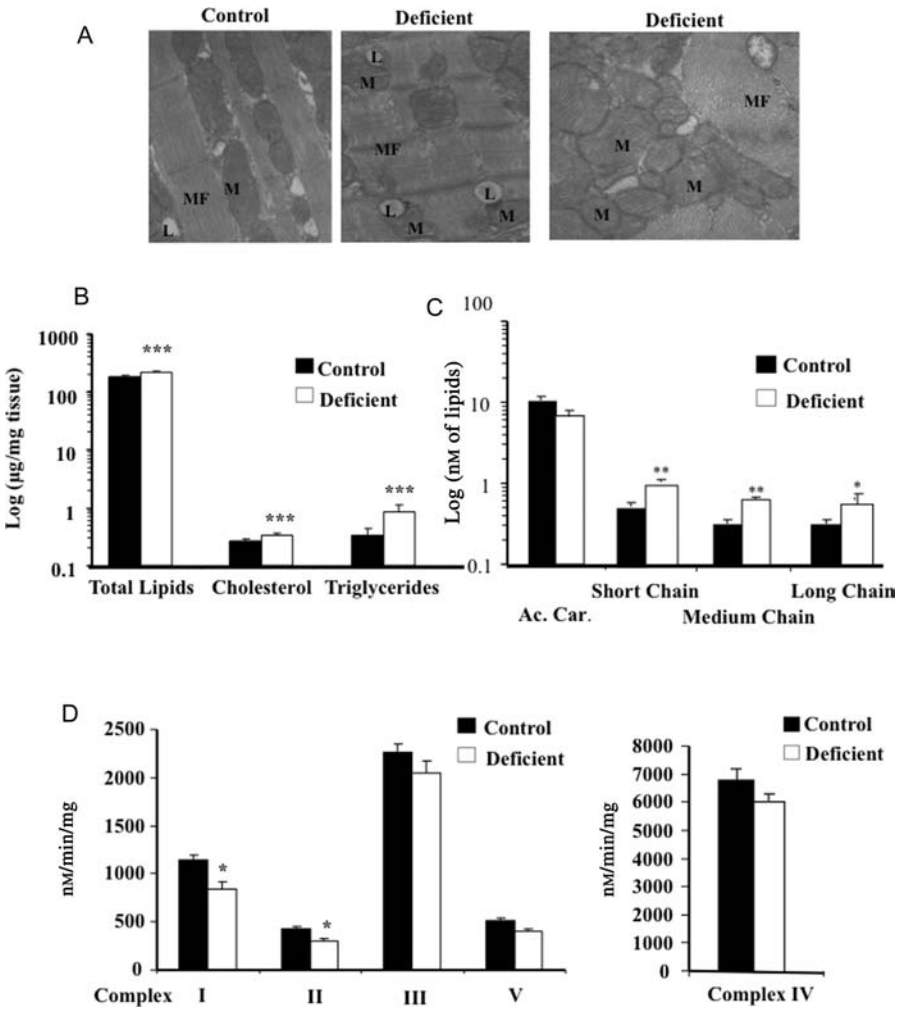

Figure 4. Consequences of the methyl-deficient diet on myocardium metabolism. (A) Electron micrographs represent sectioned left ventricles from control and methyl-deficient rats. Lipid droplets (L), mitochondria (M) and myofibrils (MF) are indicated. (B) Tissue concentrations of total lipids, cholesterol and triglycerides, $^{***}p < 0.001$. (C) Plasma acylcarnitine profiles from control and methyl-deficient rats, $n = 20$ in each group. car., carnitine; ac., acetyl. Means ± SEM, $n = 20$ in each group, $^{*}p < 0.05$, $^{**}p < 0.01$. (D) Activities of complexes I–V in mitochondria from control and methyl-deficient rats. Activities are expressed as mean ± SEM, $n = 8$ in each group, $^{*}p < 0.05$.

model [10,14]. The cardiomyopathy was documented by thickening of the myocardial walls and cardiomyocyte enlargement, in the absence of fibrosis and systolic dysfunction, in contrast to what has been observed in adult rats with hyperhomocysteinaemia produced by an homocystine-enriched diet [28]. The role of the deficiency in producing the myocardium hypertrophy was ascertained by a significant correlation of heart/body weight with folate, vitamin B12 and Hcy. The diet produced a decreased concentration of folate, a decreased SAM : SAH ratio and an increased immunohistochemical detection of Hcy in the myocardium of the deficient animals. The decreased SAM : SAH ratio was the consequence of a trap where the impaired remethylation pathway and the absence of cystathionine-ß-synthase produced a conversion of homocysteine into SAH by the reversible enzyme SAH hydrolase (see Supporting information, Figure S1) [4]. In comparison, significant elevations of Hcy have been observed in the hearts of genetic models of mice with severely elevated plasma Hcy, but not in mice fed a high-methionine diet with mildly elevated plasma Hcy [29]. Beside the tissue effects of homocysteine, the decreased SAM : SAH ratio acts on the methylation of proteins involved in epigenetic-related mechanisms, which play a key role in regulating fuel homeostasis of the myocardium during the perinatal period of life [3,4].

The disruption of the alignment of the mitochondria and the increased tissue concentration of lipids were evocative of a dramatic effect of the deficiency on the mitochondrial energy metabolism. This was also illustrated by the accumulation of lipid droplets neighbouring the mitochondria, the decreased activities of complexes I and II and altered expression of two enzymes of these complexes, NDUFV2 and NDUFA10, and the development of the cardiac hypertrophy after birth, when fatty acids are the main providers of energy to the heart [13]. Acetyl-CoA carboxylase (ACC) catalyses the synthesis of malonyl-CoA, which is the limiting substrate of fatty synthesis that directly controls the activity of CPT. Our data indicated that this pathway was not increased, since

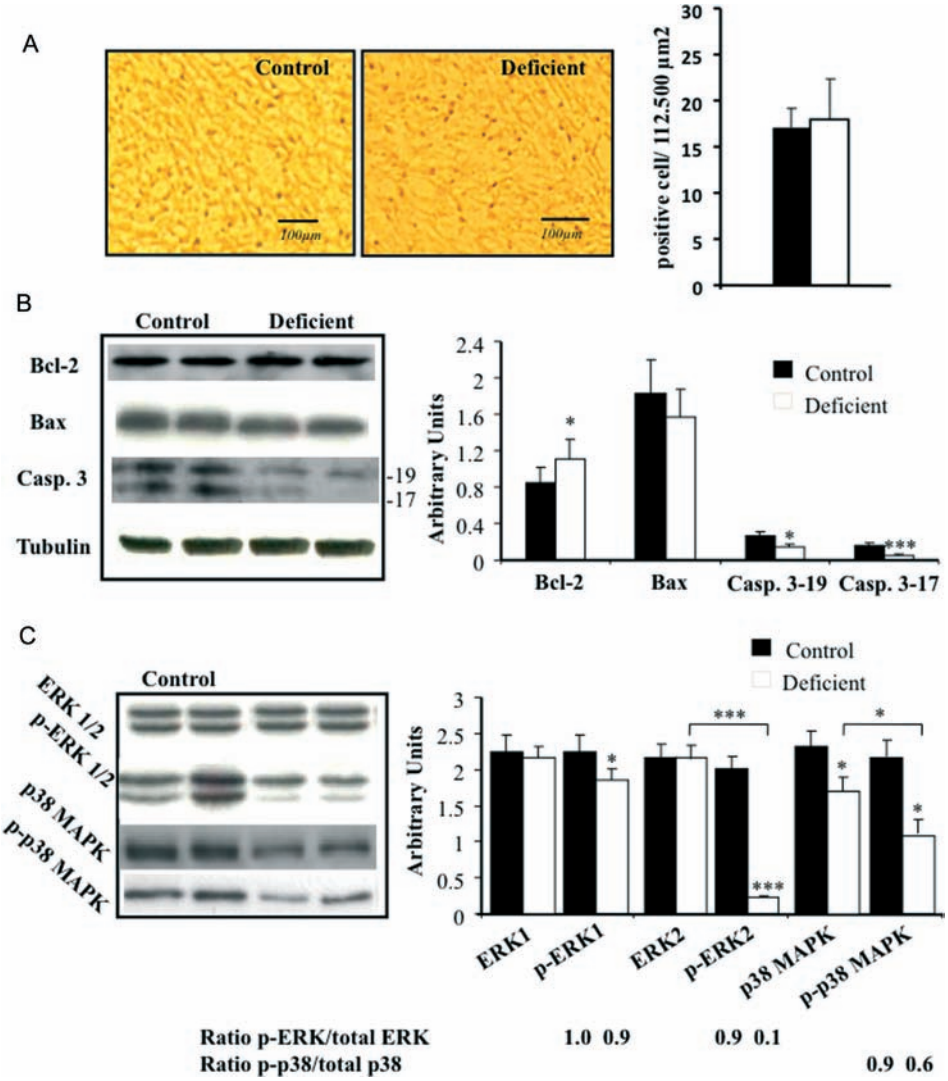

Figure 5. Influence of the methyl-deficient diet on cellular stress and apoptosis in myocardium. (A) Terminal deoxynucleotidyl transferase-mediated dUTP nick-end labelling (TUNEL) assay (left) and quantification of apoptotic cells (right); $n = 6$, mean ± SEM. (B) Examples of western blots of protein markers of apoptosis in control and methyl-deficient rats. The protein bands were quantified densitometrically and normalized to the expression of cardiac tubulin in the same sample and expressed as arbitrary units; $n = 8$ in each group, mean ± SEM. (C) Examples of western blots of ERK1/2, phosphorylated ERK1/2 (p-ERK1/2), p38-MAPK and phosphorylated p38-MAPK (p-p38). Protein bands were quantified densitometrically, normalized to the total protein content in the samples and expressed as arbitrary units; the ratios of phospho-ERK to ERK and phospho-p38-MAPK to p38-MAPK were calculated from densitometry. The values reported in deficient condition were expressed as a fraction of the ratios calculated respectively for phospho-ERK1 to ERK1 and phospho-p38 to p38 in the control condition, which were arbitrarily set as 1; $n = 8$ in each group, $^{*}p < 0.05$, $^{**}p < 0.01$, $^{***}p < 0.001$.

we did not observe any change in CPT1 activity in the deficient animals [30]. The proteomic analysis also evidenced a modified expression of proteins involved in fatty acid β-oxidation and lipid storage. MTPA, SCAD and Hspd1 protein are key proteins of fatty acid oxidation in mitochondria. Despite a moderate reduction of their expression under the influence of the methyl donor deficiency, the decreased MTPA and SCAD had significant consequences on myocardium fatty acid oxidation, as evidenced by the increased concentration of long-chain, medium-chain and short-chain acylcarnitines. This may be due to the cumulative consequences of the reduced expression of the two proteins, at the entrance and at a key downstream step of fatty acid oxidation, respectively (Figure 4; see also Supporting information, Figure S5). Hspd1 is a chaperone involved in the folding of the medium-chain acyl-CoA dehydrogenase [31].

Among the proteins with altered expression evidenced in the proteomic and western blot analyses, MTPA, NDUFA10 and FABP3 have been directly implicated in the patho-mechanisms of cardiomyopathies in previous studies [32–35]. MTPA is part of the octameric mitochondrial trifunctional protein (MTP) that catalyses the final three steps of mitochondrial fatty acid β-oxidation. $Mtpa^{-/-}$ pups develop a severe cardiomyopathy after birth and, similarly to rats deficient in methyl donors, an increased plasma level of the three groups of acylcarnitines [32]. Interestingly, a recent proteomic study of a hypertensive rat model showed that the two proteins exhibiting the most

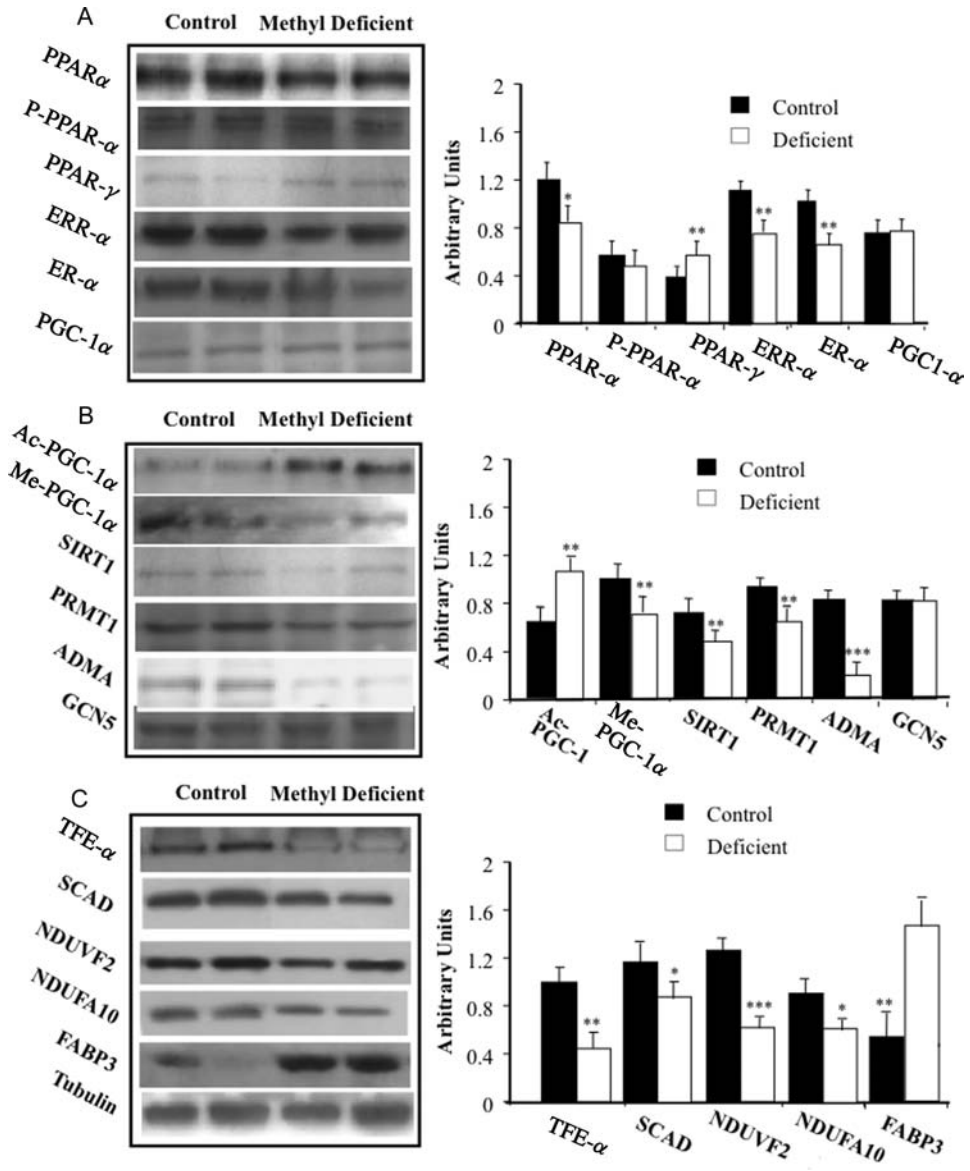

Figure 6. Effects of the methyl-deficient diet on proteins related with impaired fatty acid oxidation in rat myocardium. (A) Example of western blots of nuclear receptors and their co-activators. (B) Methylation and acetylation pathways of the PGC1-α co-activator by immunoprecipitation and western blot. (C) Example of western blots of trifunctional enzyme subunit α-complex (TFE-α), short chain acylCoA dehydrogenase (SCAD), NADH dehydrogenase (ubiquinone) flavoprotein 2 (NDUFV2), NADH dehydrogenase (ubiquinone) 1α subunit 10 (NDUFA10) and fatty acid binding protein-3 (FABP3). The protein bands of (A–C) were quantified densitometrically and expressed as arbitrary units; $n = 8$ in each group, means ± SEM, $^{*}p < 0.05$, $^{**}p < 0.01$, $^{***}p < 0.001$.

significant change in relation to myocardium hypertrophy were MTP and NDUFA10, the two proteins that also had the greatest change in our model of deficient pups (Figure 6) [33]. In this study, the altered expression of these two mitochondrial enzymes contributed to cardiac hypertrophy before the occurrence of hypertension [33]. It may be also assumed that the altered expression of NDUFV2 plays a prominent role in the myocardium hypertrophy of the deficient rats, since a mutation in this subunit of mitochondrial complex I causes early-onset hypertrophic cardiomyopathy [34]. The increased expression of FABP3, the heart-specific FABP, may also participate to the consequences of the methyl-deficient diet on myocardium by exerting harmful effects in the intracellular metabolism of fatty acids and via a high-affinity plasma membrane receptor [35].

PGC1α, PPARα and ERRα were the strongest determinants of the changes produced by the methyl-deficient diet in the bioinformatics analysis of proteomic data. Deacetylation and methylation of PGC-1α are two key regulatory mechanisms of oxidative metabolism that had a particular interest in our experimental model, where altered methylation and acetylation would be expected in the context of decreased SAM : SAH ratio and intra-uterine growth retardation [3,4]. PGC-1α function is induced through methylation at several arginine residues in the C-terminal region by protein arginine methyltransferase-I (PRMT1) [36]. The acetylation of PGC-1α decreases its activity and is regulated by the histone deacetylase SIRT1 and the

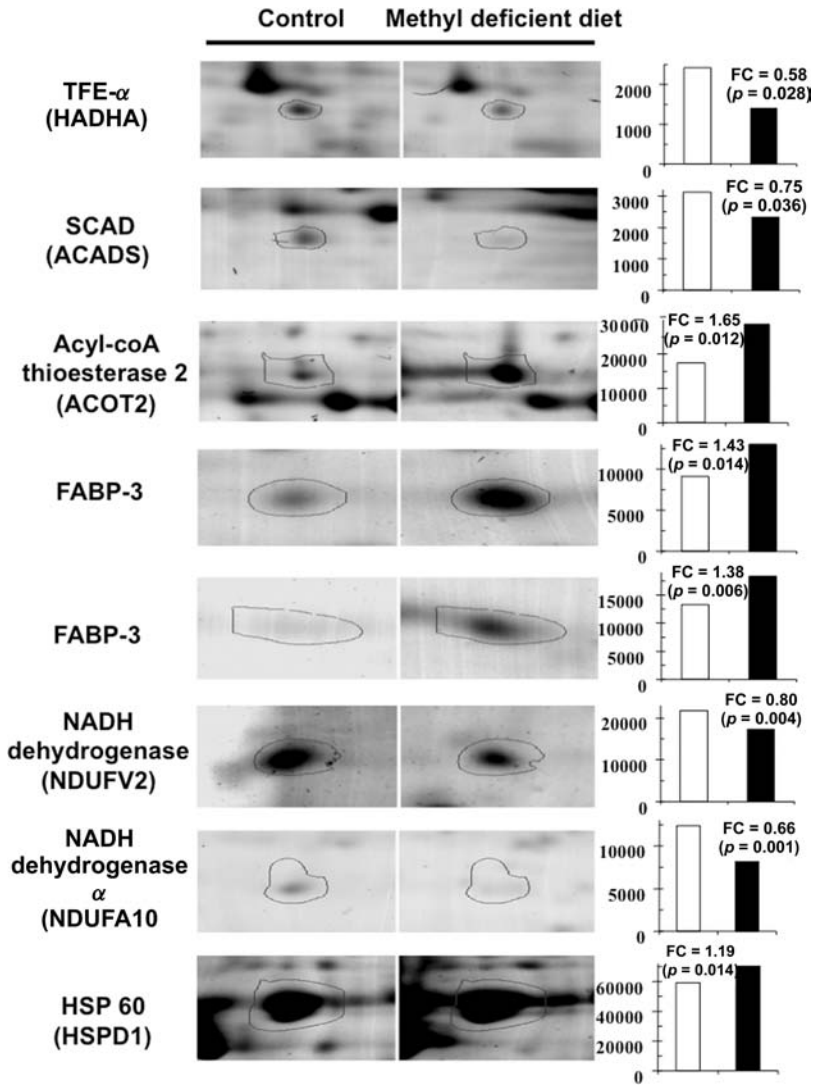

Figure 7. Proteomic analysis of myocardium from methyl-deficient and control rat pups. Magnification of spots matching myocardial proteins related with energy metabolism (abbreviations in parenthesis are the gene names), with significantly different abundance between deficient pups and controls. FC, fold change (ratio deficient versus control pups) with indication of statistical significance (*p* value); *y* axis, arbitrary units.

acetyltransferase GCN5 [3,36,37]. We have evidenced an increased acetylation and a decreased methylation of PGC-1α in the myocardium of the deficient animals. These two post-translational changes were consistent with the decreased SAM : SAH ratio and the decreased expression of SIRT1 and of PRMT1 in the deficient rats and were indicative of a functional deactivation of PGC-1α (see Supporting information, Figure S1) [3,13,37]. Similarly, the reduced protein expression of SIRT1 has been observed in skeletal muscle of pups from mothers under protein restriction [37]. This raises the hypothesis of a metabolic programming of methyl donor restriction in the heart, yet to be explored, which could be influenced by SIRT1 and PRMT1 [3,13,37,38]. The decreased protein expression of PPARα and ERRα in the myocardium of the deficient animals, in addition to the decreased activation of their co-regulator, was similarly consistent with the decreased expression of mitochondrial enzymes involved in fatty acid oxidation, including trifunctional enzyme subunit-α, short chain acylCoA dehydrogenase and FABP3 [18–26,39]. Besides the role of the decreased SAM : SAH ratio in the impaired activation of PGC-1α, the increased tissue accumulation of Hcy could participate in reducing the expression of PPARα, as previously shown in monocytes, HepG2 cells and liver tissue [40,41].

In conclusion, methyl donor deficiency had detrimental consequences on myocardium by decreasing the expression of mitochondrial enzymes involved in fatty acid oxidation and complexes I and II of respiration, through imbalanced acetylation/methylation of PGC1α by SIRT1 and PRMT1 and altered expression of PPARα and ERRα. Consequently, it should be clinically evaluated as a potential causal and/or aggravating metabolic condition of perinatal cardiomyopathies.

Acknowledgment

The authors thank Nicolas Gérard and Christophe Chambon (Human Nutrition Unit of INRA-Theix) for

performing the two-dimensional gel electrophoresis and mass spectrometry analyses, respectively. This study was supported by the Region Lorraine and by a grant from the National Agency for Research (ANR Nutrivigène) and by grants from the National Agency for Research (ANR Nutrivigène) and from the fondation pour la recherche médicale.

Author contributions

JLG, RMGR and PB conceived the study, JLG, MM, PB and RMGR wrote the manuscript, MM, SP, PB, JMA, EJ, FM, GN carried out experiments, JLG, RMGR, MM, PB, PYM, PL, YJ and YM analysed data. All authors had final approval of the submitted and published versions.

Abbreviations

ACOT, acyl-coenzyme A thioesterase; ADMA, asymmetric dimethylarginine; Cbl, cobalamin; CPT, carnityl palmitoyl transferase; NAD, nicotinamide adenine dinucleotide; ERK, extracellular signal-regulated kinase; ERRα, oestrogen-related receptor-α; FABP, fatty acid binding protein; GPX, glutathione peroxidase; HF, heart failure; Hcy, homocysteine; HADHA, hydroxyacyl-CoA dehydrogenase/3-ketoacyl-CoA thiolase/enoyl-CoA hydratase (trifunctional protein), alpha subunit; HSP, heat shock protein; IDH, isocitrate dehydrogenase; LC–MS/MS, liquid chromatography–tandem mass spectrometry; LVEF, left ventricular ejection fraction; MAPK, mitogen-activated protein kinase; MDA, malondialdehyde; MTHFR, methylenetetrathydrofolate reductase; MTP, mitochondrial trifunctional protein; MTR, methionine synthase; NDUFA10, NADH dehydrogenase (ubiquinone) 1α subunit 10; NDUFV, NADH dehydrogenase (ubiquinone) flavoprotein 2; NT-proBNP, plasma N-terminal-prohormone-brain natriuretic peptide; OCTN, novel organic cation transporter; PET, positron emission tomography; PGC-1α, PPAR-γ co-activator-1α; PPAR, peroxisome proliferator-activated receptor; PRMT, protein arginine methyltransferase; SAH, *S*-adenosylhomocysteine; SAM, *S*-adenosylmethionine; SCAD, short chain acylCoA dehydrogenase; SIRT, sirtuin; SOD, superoxide dismutase; TFE-α, trifunctional enzyme subunit-α complex; TUNEL, terminal deoxynucleotidyl transferase-mediated dUTP nick-end labelling.

References

1. Jessup M, Brozena S. Heart failure. *N Engl J Med* 2003; **348**: 2007–2018.
2. Charron P, Arad M, Arbustini E, *et al*. Genetic counselling and testing in cardiomyopathies: a position statement of the European Society of Cardiology Working Group on Myocardial and Pericardial Diseases. *Eur Heart J* 2010; **31**: 2715–2726.
3. Holness MJ, Caton PW, Sugden MC. Acute and long-term nutrient-led modifications of gene expression: potential role of SIRT1 as a central co-ordinator of short and longer-term programming of tissue function. *Nutrition* 2010; **26**: 491–501.
4. Forges T, Monnier-Barbarino P, Alberto JM, *et al*. Impact of folate and homocysteine metabolism on human reproductive health. *Hum Reprod Update* 2007; **13**: 225–238.
5. Spada RS, Stella G, Calabrese S, *et al*. Association of vitamin B12, folate and homocysteine with functional and pathological characteristics of the elderly in a mountainous village in Sicily. *Clin Chem Lab Med* 2007; **45**: 136–142.
6. De Bie I, Nizard SD, Mitchell GA. Fetal dilated cardiomyopathy: an unsuspected presentation of methylmalonic aciduria and hyperhomocystinuria, cblC type. *Prenat Diagn* 2009; **29**: 266–270.
7. Gueant-Rodriguez RM, Juilliere Y, Nippert M, *et al*. Left ventricular systolic dysfunction is an independent predictor of homocysteine in angiographically documented patients with or without coronary artery lesions. *J Thromb Haemost* 2007; **5**: 1209–1216.
8. Herrmann W, Herrmann M, Joseph J, *et al*. Homocysteine, brain natriuretic peptide and chronic heart failure: a critical review. *Clin Chem Lab Med* 2007; **45**: 1633–1644.
9. Chen P, Poddar R, Tipa EV, *et al*. Homocysteine metabolism in cardiovascular cells and tissues: implications for hyperhomocysteinemia and cardiovascular disease. *Adv Enzyme Regul* 1999; **39**: 93–109.
10. Blaise SA, Nedelec E, Schroeder H, *et al*. Gestational vitamin B deficiency leads to homocysteine-associated brain apoptosis and alters neurobehavioral development in rats. *Am J Pathol* 2007; **170**: 667–679.
11. Chanson A, Rock E, Martin JF, *et al*. Preferential response of glutathione-related enzymes to folate-dependent changes in the redox state of rat liver. *Eur J Nutr* 2007; **46**: 204–212.
12. Battaglia-Hsu SF, Akchiche N, Noel N, *et al*. Vitamin B12 deficiency reduces proliferation and promotes differentiation of neuroblastoma cells and up-regulates PP2A, proNGF, and TACE. *Proc Natl Acad Sci USA* 2009; **106**: 21930–21935.
13. Ventura-Clapier R, Garnier A, Veksler V. Transcriptional control of mitochondrial biogenesis: the central role of PGC-1α. *Cardiovasc Res* 2008; **79**: 208–217.
14. Bossenmeyer-Pourié C, Blaise S, Pourié G, *et al*. Methyl donor deficiency affects fetal programming of gastric ghrelin cell organization and function in the rat. *Am J Pathol* 2010; **176**: 270–277.
15. Madrazo JA, Kelly DP. The *PPAR* trio: regulators of myocardial energy metabolism in health and disease. *J Mol Cell Cardiol* 2008; **44**: 968–975.
16. Briand G, Fontaine M, Schubert R, *et al*. Direct analysis by electrospray ionization and matrix-assisted laser desorption ionization mass spectrometry of standard and urinary acylcarnitines. Comparison with fast atom bombardment and gas chromatography chemical ionization mass spectrometry. *J Mass Spectrom* 1995; **30**: 1731–1741.
17. Johnson G, Roussel D, Dumas JF, *et al*. Influence of intensity of food restriction on skeletal muscle mitochondrial energy metabolism in rats. *Am J Physiol Endocrinol Metab* 2006; **291**: E460–467.
18. Chang YI, Hua WK, Yao CL, *et al*. Protein–arginine methyltransferase 1 suppresses megakaryocytic differentiation via modulation of the p38 MAPK pathway in K562 cells. *J Biol Chem* 2010; **285**: 20595–20606.
19. Aoyama T, Peters JM, Iritani N, *et al*. Altered constitutive expression of fatty acid-metabolizing enzymes in mice lacking the peroxisome proliferator-activated receptor-α (PPARα). *J Biol Chem* 1998; **273**: 5678–5684.
20. Liu YY, Heymann RS, Moatamed F, *et al*. A mutant thyroid hormone receptor-α antagonizes peroxisome proliferator-activated

receptor-α signaling *in vivo* and impairs fatty acid oxidation. *Endocrinology* 2007; **148**: 1206–1217.
21. Qiu L, Wu X, Chau JF, *et al*. Aldose reductase regulates hepatic peroxisome proliferator-activated receptor-α phosphorylation and activity to impact lipid homeostasis. *J Biol Chem* 2008; **283**: 17175–17183.
22. Sandri M, Lin J, Handschin C, *et al*. PGC-1α protects skeletal muscle from atrophy by suppressing FoxO3 action and atrophy-specific gene transcription. *Proc Natl Acad Sci USA* 2006; **103**: 16260–16265.
23. Schachtrup C, Emmler T, Bleck B, *et al*. Functional analysis of peroxisome-proliferator-responsive element motifs in genes of fatty acid-binding proteins. *Biochem J* 2004; **382**: 239–245.
24. Kawabe K, Saegusa H, Seto K, *et al*. Peroxisome proliferator-activated receptor-α and its response element are required but not sufficient for transcriptional activation of the mouse heart-type fatty acid binding protein gene. *Int J Biochem Cell Biol* 2005; **37**: 1534–1546.
25. Stavinoha MA, RaySpellicy JW, Essop MF, *et al*. Evidence for mitochondrial thioesterase 1 as a peroxisome proliferator-activated receptor-α-regulated gene in cardiac and skeletal muscle. *Am J Physiol Endocrinol Metab* 2004; **287**: E888–895.
26. Huss JM, Torra IP, Staels B, *et al*. Estrogen-related receptor-α directs peroxisome proliferator-activated receptor-α signaling in the transcriptional control of energy metabolism in cardiac and skeletal muscle. *Mol Cell Biol* 2004; **24**: 9079–9091.
27. Chen HS, Wu TE, Juan CC, *et al*. Myocardial heat shock protein 60 expression in insulin-resistant and diabetic rats. *J Endocrinol* 2009; **200**: 151–157.
28. Devi S, Kennedy RH, Joseph L, *et al*. Effect of long-term hyperhomocysteinemia on myocardial structure and function in hypertensive rats. *Cardiovasc Pathol* 2006; **15**: 75–82.
29. Jakubowski H, Perla-Kaján J, Finnell RH, *et al*. Genetic or nutritional disorders in homocysteine or folate metabolism increase protein *N*-homocysteinylation in mice. *FASEB J* 2009; **23**: 1721–1727.
30. Folmes CD, Lopaschuk GD. Role of malonyl-CoA in heart disease and the hypothalamic control of obesity. *Cardiovasc Res* 2007; **73**: 278–287.
31. Corydon TJ, Hansen J, Bross P, *et al*. Down-regulation of Hsp60 expression by RNAi impairs folding of medium-chain acyl-CoA dehydrogenase wild-type and disease-associated proteins. *Mol Genet Metab* 2005; **85**: 260–270.
32. Ibdah JA, Paul H, Zhao Y, *et al*. Lack of mitochondrial trifunctional protein in mice causes neonatal hypoglycemia and sudden death. *J Clin Invest* 2001; **107**: 1403–1409.
33. Meng C, Jin X, Xia L, *et al*. Alterations of mitochondrial enzymes contribute to cardiac hypertrophy before hypertension development in spontaneously hypertensive rats. *J Proteome Res* 2009; **8**: 2463–2475.
34. Bénit P, Beugnot R, Chretien D, *et al*. Mutant NDUFV2 subunit of mitochondrial complex I causes early onset hypertrophic cardiomyopathy and encephalopathy. *Hum Mutat* 2003; **21**: 582–586.
35. Lamounier-Zepter V, Look C, Alvarez J, *et al*. Adipocyte fatty acid-binding protein suppresses cardiomyocyte contraction: a new link between obesity and heart disease. *Circ Res* 2009; **105**: 326–334.
36. Teyssier C, Ma H, Emter R, *et al*. Activation of nuclear receptor coactivator PGC-1α by arginine methylation. *Genes Dev* 2005; **19**: 1466–1473.
37. Jeninga EH, Schoonjans K, Auwerx J. Reversible acetylation of PGC-1: connecting energy sensors and effectors to guarantee metabolic flexibility. *Oncogene* 2010; **29**: 4617–4624.
38. Chen JH, Martin-Gronert MS, Tarry-Adkins J, *et al*. Maternal protein restriction affects postnatal growth and the expression of key proteins involved in lifespan regulation in mice. *PLoS One* 2009; **4**: e4950.
39. Huss JM, Imahashi K, Dufour CR, *et al*. The nuclear receptor ERRα is required for the bioenergetic and functional adaptation to cardiac pressure overload. *Cell Metab* 2007; **6**: 25–37.
40. Mikael LG, Genest J, Jr., Rozen R. Elevated homocysteine reduces apolipoprotein A-I expression in hyperhomocysteinemic mice and in males with coronary artery disease. *Circ Res* 2006; **98**: 564–571.
41. Yideng J, Zhihong L, Jiantuan X, *et al*. Homocysteine-mediated PPARα,γ DNA methylation and its potential pathogenic mechanism in monocytes. *DNA Cell Biol* 2008; **27**: 143–150.
42. *Holness MJ, Caton PW, Sugden MC. Acute and long-term nutrient-led modifications of gene expression: potential role of SIRT1 as a central co-ordinator of short and longer-term programming of tissue function. *Nutrition* 2010; **26**: 491–501.
43. *Johnson G, Roussel D, Dumas JF, *et al*. Influence of intensity of food restriction on skeletal muscle mitochondrial energy metabolism in rats. *Am J Physiol Endocrinol Metab* 2006; **291**: E460–467.

* These references are cited in the Supporting information only.

SUPPORTING INFORMATION ON THE INTERNET

The following supporting information may be found in the online version of this article:

Figure S1. One-carbon metabolism and the consequences of the methyl-deficient diet on the myocardium of rats.

Figure S2. Influence of the methyl donor deficient diet on carnitine palmitoyltransferase 1 (CTP1) activity.

Figure S3. Influence of the methyl donor-deficient diet on SIRT1 activity.

Figure S4. Ingenuity pathways analysis (IPA) of the proteomic data related to fatty acid oxidation and energy metabolism in myocardium.

Figure S5. Metabolic chart of fatty acid oxidation and respiratory chain and protein changes produced by the methyl donor-deficient diet.